

Article

Recovery of Elemental Arsenic from Acidic As-Containing Wastewater by a Hypophosphite Reduction Process

Qian Li ¹, Shiyu Zhao ¹, Yan Zhang ^{1,*} , Yong Li ¹, Xiaoliang Liu ²  and Yongbin Yang ¹

¹ School of Minerals Processing and Bioengineering, Central South University, Changsha 410083, China; csuliqian@126.com (Q.L.); 215612107@csu.edu.cn (S.Z.); 15037170829@163.com (Y.L.); ybyangcsu@126.com (Y.Y.)

² Changsha Research Institute of Mining and Metallurgy Co., Ltd., Changsha 410012, China; xiaoliang_liu6369@163.com

* Correspondence: yanzhang301527@163.com

Abstract: Biological oxidation is a low-carbon technology for the treatment of As-containing gold ores, but it causes a large amount of acidic As-containing wastewater that is harmful to the environment. This paper proposed a novel, eco-friendly method to treat this wastewater. Thermodynamic analysis, H_2PO_2^- reduction, and wastewater recycling tests were conducted. Thermodynamic analysis indicates the feasibility of the reduction of As(V)/As(III) by H_2PO_2^- or H_3PO_2 to As^0 under acidic conditions. Experimental results confirmed the thermodynamic prediction and showed that H_2PO_2^- could efficiently convert the As (i.e., As(V)/As(III)) in the wastewater to high value-added As^0 . Under the optimal conditions, 99.61% of As precipitated out, and the obtained As^0 had a high purity of 98.5%. Kinetic results showed that the reaction order of H_2PO_2^- concentration was 0.6399, and the activation energy of the H_2PO_2^- reduction process was 34.33 kJ/mol, which is indicative of a mixed-controlled process (20–40 kJ/mol). Wastewater recycling results showed that after recovering As, the wastewater could be reused as a bacterial culture medium. Based on the thermodynamic analysis and experimental and analytical results, hypophosphite reduction mechanisms for removing and recovering As from its acidic wastewater were proposed. The results presented in this paper suggest the feasibility of this one-step H_2PO_2^- reduction approach, which may be promising in treating acidic As-containing wastewater.



Citation: Li, Q.; Zhao, S.; Zhang, Y.; Li, Y.; Liu, X.; Yang, Y. Recovery of Elemental Arsenic from Acidic As-Containing Wastewater by a Hypophosphite Reduction Process. *Water* **2024**, *16*, 1301. <https://doi.org/10.3390/w16091301>

Academic Editor: Ondra Sracek

Received: 4 April 2024

Revised: 27 April 2024

Accepted: 29 April 2024

Published: 2 May 2024



Copyright: © 2024 by the authors. Licensee MDPI, Basel, Switzerland. This article is an open access article distributed under the terms and conditions of the Creative Commons Attribution (CC BY) license (<https://creativecommons.org/licenses/by/4.0/>).

Keywords: biological oxidation; acidic As-containing wastewater; hypophosphite; reduction; elemental arsenic

1. Introduction

Arsenic has been classified as a primary carcinogen by the International Cancer Organization [1–3]. In aqueous environments, As(III) and As(V) exist predominantly as inorganic arsenite and arsenate species, with As(III) exhibiting significantly higher toxicity and mobility compared to As(V) [4]. The contamination of the environment with arsenic has been exacerbated in recent years due to ongoing mining activities [5], smelting processes [6], the growth of the semiconductor manufacturing industry [7], and improper agrochemical applications [8]. In the gold smelting industry, biological oxidation is extensively employed for pretreating As-containing gold ores. However, this method generates substantial volumes of acidic wastewater containing high concentrations of arsenic. Effective treatment of such acidic wastewater derived from biological oxidation has emerged as a significant challenge in the gold smelting sector.

Common methods for removing arsenic from As-containing wastewater include adsorption [9], ion exchange [10], and precipitation [11–13]. The adsorption method offers the advantages of low cost, simple operation, and large adsorption capacity. However, the difficulty in recycling the adsorption material and the interference of co-existing ions greatly affect its adsorption rate. The ion exchange method is susceptible to the influence

of impurity ions. Although precipitation has the benefits of requiring less investment and being easy to operate, it also produces hazardous waste. In comparison with the adsorption, ion exchange, and precipitation methods, reduction using a reductant to convert As(V) and As(III) in As-containing wastewater into high-value-added products with stable properties and low toxicity is preferred.

There are only a few studies on the treatment of As-containing wastewater by the reduction method. The reduction method can realize the resource utilization of arsenic-containing wastewater and is a possible direction for future development. However, current research mainly focuses on the reduction of arsenic-containing wastewater with UV/reducing agents. Wang et al. [14] successfully recovered elemental arsenic by employing the UV/sulfite method to reduce As(V) and As(III) from solution. However, this method is only suitable for treating wastewater containing low As concentrations. Although this method can achieve the reduction of As(III)/As(V) in acidic As-containing wastewater, whether the process can treat bio-oxidation As-containing wastewater is unknown. Feng [15] used potassium borohydride (KBH_4) as a reducing agent to convert soluble arsenic into gaseous arsenic (AsH_3) or solid arsenic (As^0), achieving the goal of removing arsenic from wastewater. However, it should be noted that the generated AsH_3 is toxic. Li and Tian [16] employed a two-stage reduction process of utilizing hydrazine hydrate in the first stage and hypophosphite in the second stage to achieve a total reduction efficiency of 91.77% for converting As into its elemental form from actual As-containing wastewater. Although this two-stage reduction process allows for resource utilization of arsenic in wastewater, it should be noted that the hydrazine hydrate used in the first stage possesses certain toxicity and environmental harm [17]. Another disadvantage of the above two-stage reduction process is its complexity. Therefore, it is of great significance to seek a safe, environmentally friendly, and efficient reducing agent and develop a simple process to realize the resource utilization of acidic As-containing wastewater with minimized impact on the environment.

Hypophosphite (such as sodium hypophosphite), as a strong reducing agent, is widely used in the food industry as an antioxidant and preservative [18]. In the alloy industry, hypophosphite has the potential to replace formaldehyde to reduce high-valence metal ions to low-valence metal elements [19]. Hypophosphite has the advantages of low cost and non-toxicity. Few attempts, however, have been made to treat acidic As-containing wastewater using only hypophosphite.

In this paper, one-stage hypophosphite reduction was adopted to treat an actual acidic As-containing wastewater from the bio-oxidation pretreatment of a refractory As-containing gold ore. This study started with thermodynamic analysis to reveal the likely speciation change for the As, P, and Fe species in acidic As-containing wastewater and thus predict the theoretical possibility of recovering As from its acidic wastewater as As^0 by hypophosphite reduction. An in-depth investigation into the effect of influencing factors on the reduction efficiency of As by hypophosphite was then performed. The recycling of the wastewater after hypophosphite reduction as a culture medium was also investigated. Finally, the relevant hypophosphite reduction mechanisms for As recycling from the acidic As-containing wastewater were elucidated. This paper offers a novel eco-friendly one-stage hypophosphite reduction technology that may be promising for the treatment of acidic As-containing wastewater, particularly in the bio-hydrometallurgy industry.

2. Materials and Methods

2.1. Experimental Materials

The acidic As-containing wastewater used in all experiments was the bioleaching solution of a refractory As-containing gold ore (As 19.32%) after 14 days of bio-oxidation pretreatment by *Acidithiobacillus ferrooxidans* (*A. ferrooxidans*). The *A. ferrooxidans* were from the Key Laboratory of Biometallurgy, Ministry of Education of China (Changsha, China). This wastewater has strong acidity ($\text{pH} \approx -0$). Table 1 shows that it mainly consisted of

As 2.532 g/L and Fe 5.594 g/L, of which the As included As³⁺ and As⁵⁺ and the Fe was mainly Fe³⁺ [20–22].

Table 1. The content of main components in bio-oxidation leaching solution.

Element	Fe ²⁺	Fe ³⁺	As ³⁺	As ⁵⁺
Content (g/L)	0.231	5.363	1.647	0.876

The reagents used in the hypophosphite reduction experiments and the cultivation of bacteria were all analytical reagent grade. De-ionized water was used throughout all experiments.

2.2. Experimental Methods

The unsterilized bioleaching solution, i.e., As-containing wastewater (500 mL), was added to a closed container, and then the As-containing wastewater was purged with nitrogen (N₂) for 30 or 180 min to remove the dissolved oxygen (O₂) to different O₂ concentration levels (38.0 mg/L, 8.5 mg/L, and 1.2 mg/L). After the constant-temperature water bath was heated to the reaction temperature, the stirrer was opened, and the rotation speed was adjusted to 300 rpm. Then a certain amount of sodium hypophosphite was added to the As-containing wastewater, and the solution pH value was quickly adjusted by the careful addition of ~0.01 mol/L H₂SO₄ or NaOH solution. Each reduction test started once the solution pH was adjusted well. During the reduction test, 1 mL of the sample was taken at an interval of 30 min for chemical analysis. After each reduction test was completed, the sample was filtrated through a filter membrane with a pore size of 0.45 μm to separate the solution and the solid product for chemical analysis and characterization. Before the characterization of the solid product, it was dried in a vacuum oven at 35 °C overnight.

After removing the As, the wastewater was reused as a culture medium for *A. ferrooxidans*. In the wastewater recycling tests, the initial pH of the wastewater was adjusted to 2.0 ± 0.05 with H₂SO₄ or NaOH solution before the culture of *A. ferrooxidans*. The conventional 9K culture medium was used as the standard to evaluate the effect of the wastewater on the growth of *A. ferrooxidans*. More details can be found in our previous study [20].

2.3. Analytical Methods

The dissolved oxygen concentration in solution was determined by a dissolved oxygen tester (Shanghai LeiCi, JPBJ-611Y, Shanghai, China). The total arsenic concentration in solution was determined by inductively coupled plasma-atomic emission spectrometry (ICP-OES, ICAP7400 Radial, Thermo Fisher Scientific, Waltham, MA, USA). The arsenic reduction efficiency is calculated as shown in Equation (1). The arsenic content of the solid sample was determined by the first dissolution of the solid sample using a NaOH solution and then ICP-OES (Equation (2)).

$$A = \frac{(BV - CV)}{BV} \times 100\% \quad (1)$$

A: As reduction efficiency (%)

B: As concentration of original acidic wastewater (g/L)

C: As concentration of reduced solution (g/L)

V: acid wastewater volume (L)

$$A = \frac{CV}{B \times 10^6} \times 100\% \quad (2)$$

A: purity of As (%)

B: solid mass (g)

C: arsenic concentration in solution (g/L)

V: solution volume (L)

The concentrations of total soluble iron ($[\text{Fe}^{\text{T}}]_{\text{aq}}$) and Fe^{3+} ($[\text{Fe}^{3+}]_{\text{aq}}$) during hypophosphite reduction were determined using the 5-sulfosalicylic acid colorimetric method [23]. $[\text{Fe}^{2+}]_{\text{aq}}$ was measured using the ferrozine method [24]. The lattice structure of the solid product was measured by X-ray diffraction (XRD; D8 ADVANCE, Bruker, Berlin, Germany).

The number of bacteria in the bacterial solution was directly counted with a binocular electron microscope and blood cell counting plate. At regular intervals, microscopic counting of *A. ferrooxidans* cultured in different liquids was performed. The cultured bacteria droplets were taken on the blood cell counting plate to observe several typical areas. The number of living bacteria in each region was recorded, averaged, and multiplied by 4×10^6 to obtain the number of bacteria at some time point.

3. Results and Discussion

3.1. Thermodynamic Analysis

Based on the main composition of the acidic As-containing wastewater with high acidity ($\text{pH} \approx 0$) and high solution potential ($E_h \approx 860$ mV), HYDRA-MEDUSA software (version 16.1) was used to construct the Eh-pH diagram (Figure 1) of the As-Fe- H_2PO_2^- - H_2O system to present the Eh-pH predominance areas for the As, Fe, and P species under acidic conditions (pH from -2 to 2). Thermodynamic analysis on relevant redox couples was conducted to predict the theoretical possibility of the redox reactions among these species. It should be noted that the thermodynamic data used for calculation were from the Hydrochemical log K Database of the HYDRA module. All solution potentials were reported relative to the standard hydrogen electrode (SHE).

Figure 1a,b shows that the predominance areas of As and Fe species at pH of -2 – 2 and E_h of ~ 860 mV are H_3AsO_4 and Fe^{3+} , respectively, which is consistent with the solution composition (Table 1). In addition, the redox couples of $\text{H}_3\text{AsO}_4/\text{H}_2\text{AsO}_2^+$ (equilibrium potential $E_h^0 = 725$ – 580 mV) at pH of -2 – -0.3 , $\text{H}_3\text{AsO}_4/\text{H}_3\text{AsO}_3$ ($E_h^0 = 580$ – 100 mV) at pH of -0.3 – 2 , $\text{H}_2\text{AsO}_2^+/\text{As}^0$ ($E_h^0 = 300$ – 230 mV) at pH of -2 – -0.3 , and $\text{H}_3\text{AsO}_3/\text{As}^0$ ($E_h^0 = 230$ – 100 mV) at pH of -0.3 – 2 for As species, and $\text{Fe}^{3+}/\text{Fe}^{2+}$ ($E_h^0 = 800$ mV) and $\text{Fe}^{2+}/\text{Fe}^0$ ($E_h^0 = -480$ mV) for Fe species form at E_h scale of -1000 – 1000 mV. In terms of the acidic wastewater used in this study, its solution potential is determined by the $\text{Fe}^{3+}/\text{Fe}^{2+}$ couple [20]. The Eh-pH stability area of As^0 (Figure 1a) is completely included in that of Fe^{2+} (Figure 1b), indicating that the Fe species exist as Fe^{2+} when the As species occur in the form of As^0 .

The predominance areas of P species are shown in Figure 1c, including H_3PO_4 (P(V)), $\text{H}_3\text{PO}_3/\text{H}_2\text{PO}_2$ (P(III)), $\text{H}_3\text{PO}_2/\text{H}_2\text{PO}_2^-$ (P(I)). The species of $\text{H}_3\text{PO}_3/\text{H}_2\text{PO}_3^-$ appear unstable due to their quite narrow stability areas. A series of redox couples also form for P species, i.e., $\text{H}_3\text{PO}_4/\text{H}_3\text{PO}_3$ ($E_h^0 = -400$ – -600 mV) at pH of -2.0 – 1.5 , $\text{H}_3\text{PO}_4/\text{H}_2\text{PO}_3^-$ ($E_h^0 = -600$ – -620 mV) at pH of 1.5 – 2.0 , $\text{H}_3\text{PO}_3/\text{H}_3\text{PO}_2$ ($E_h^0 = -410$ – -610 mV) at pH of -2.0 – 1.3 , $\text{H}_2\text{PO}_3^-/\text{H}_2\text{PO}_2^-$ ($E_h^0 = -610$ – -640 mV) at pH of 1.5 – 2.0 . It is clear that the redox potentials of the P species couples are much lower than those of the As species and Fe species couples. In other words, when H_2PO_3^- was added to the acidic As-containing wastewater, thermodynamically, H_2PO_3^- reacted with H^+ to form more stable H_3PO_3 . The formed H_3PO_3 is able to reduce Fe^{3+} and H_3AsO_4 to Fe^{2+} and $\text{H}_3\text{AsO}_3/\text{H}_2\text{AsO}_2^+$, respectively, and simultaneously it is oxidized to mainly H_3PO_4 . In addition, $\text{H}_3\text{AsO}_3/\text{H}_2\text{AsO}_2^+$ can be reduced to As^0 with no reduction of Fe^{2+} to Fe^0 . Although the redox couple of $\text{O}_2/\text{H}_2\text{O}$ ($E_h^0 = 1345$ – 1107 mV at pH from -2 to 2) is not shown in Figure 1, it has much higher potential than that of the P species couples. This indicates that the dissolved oxygen (O_2) in solution has a significant influence on the stability of $\text{H}_3\text{PO}_2/\text{H}_2\text{PO}_2^-$, which is readily oxidized by O_2 to H_3PO_4 .

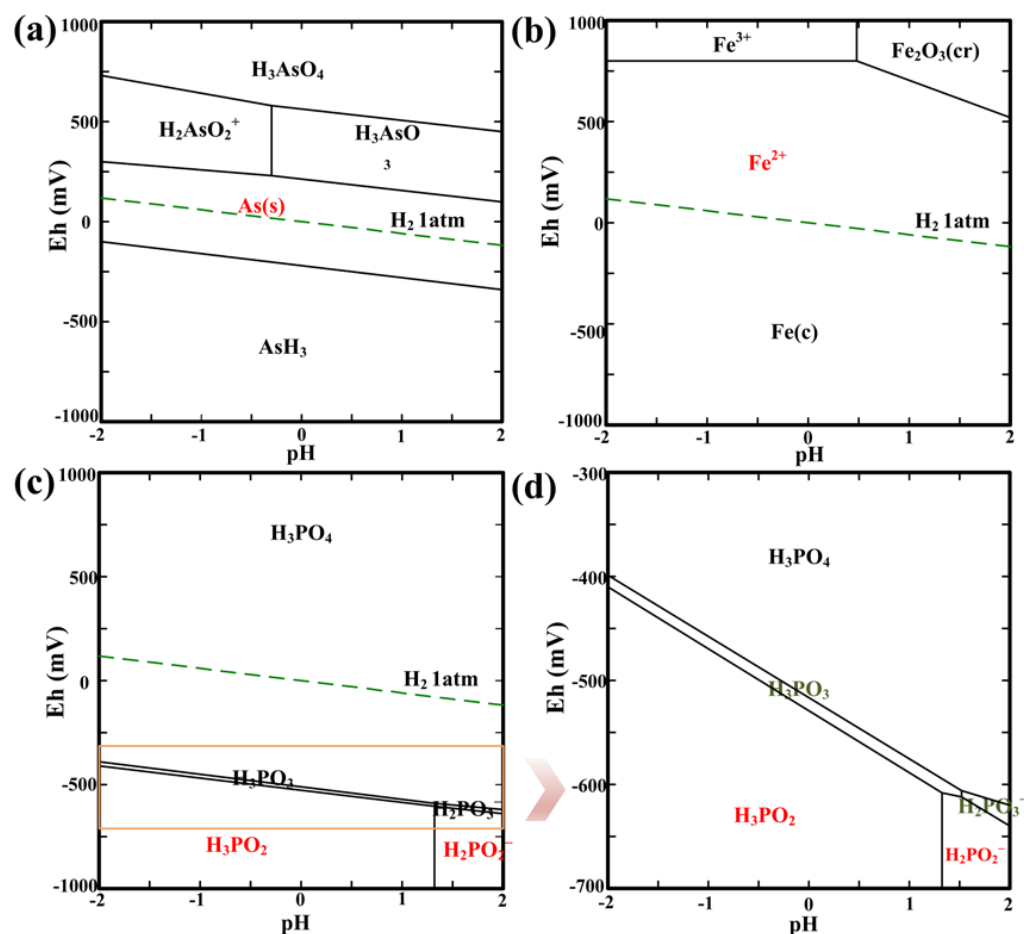


Figure 1. Eh–pH diagram of the As–Fe–H₂PO₂⁻–H₂O system showing the predominance areas of (a) As species, (b) Fe species, (c) P species and (d) partially enlarged plot of P species. Conditions: [As] 33.8 mM, [Fe] 100 mM, [PO₂³⁻] 338 mM; 25 °C, 1atm.

3.2. Recycling of As from the Acidic Wastewater by Hypophosphite Reduction

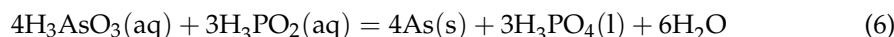
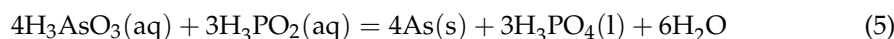
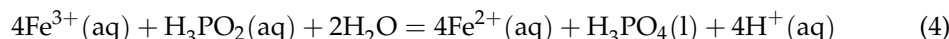
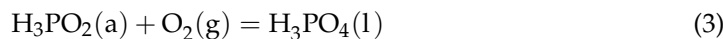
Hypophosphite reduction experiments were conducted based on the thermodynamic analysis. The effects of dissolved oxygen, hypophosphite concentration, pH, temperature, and time on As reduction efficiency were investigated.

3.2.1. Effect of Dissolved Oxygen

Due to the easy oxidation of H₃PO₂/H₂PO₂⁻ by dissolved oxygen (O₂), the influence of O₂ on the reduction of As from the wastewater using hypophosphite was investigated under the conditions of n(H₂PO₂⁻)/n(As) 5, pH 0, stirring speed 300 rpm, temperature 50 °C. The results are shown in Figure 2.

The presence of O₂ markedly influences the reduction of As (Figure 2a). Under the same dosage of H₂PO₂⁻, the As reduction efficiency was increased by around 15.33% (from 38.92% to 54.25%) when the O₂ concentration was reduced from 38.0 mg/L to 8.5 mg/L. In addition, the As reduction efficiency was further increased (from 54.25% to 66.02%) with the further decrease in O₂ concentration (<8.5 mg/L). The better As reduction achieved at a lower O₂ concentration can be explained by the fact that a lower O₂ concentration causes lower hypophosphite consumption through the reaction of (1). The solution potential (Eh) levels (Figure 2b) under high and low concentrations of O₂ (i.e., 38.0 mg/L, 1.2 mg/L) were found to both have a decreasing tendency. This is mainly due to the decrease in the Fe³⁺ oxidant (Equation (2)). The Eh level in the presence of a high O₂ concentration (38.0 mg/L) was greater than that at a low O₂ concentration (1.2 mg/L) since the O₂ itself is also an oxidant. The pH also changed during the reduction process with a downward

trend, as shown in Figure 2c. The decrease in pH is largely attributed to the formation of H^+ from the reduction of Fe^{3+} by H_3PO_2 (Equation (2)). Compared to the situation for high O_2 concentration (i.e., 38.0 mg/L), the pH level was lower than that under low O_2 concentration (i.e., 8.5 mg/L, 1.2 mg/L). The reason for this phenomenon is likely due to the oxidation of O_2 toward Fe^{2+} , where H^+ is consumed, as shown by Equation (5).



The Gibbs free energy of the above reactions was calculated by HSC6.0 software. The results show that the reactions can be spontaneous at room temperature.

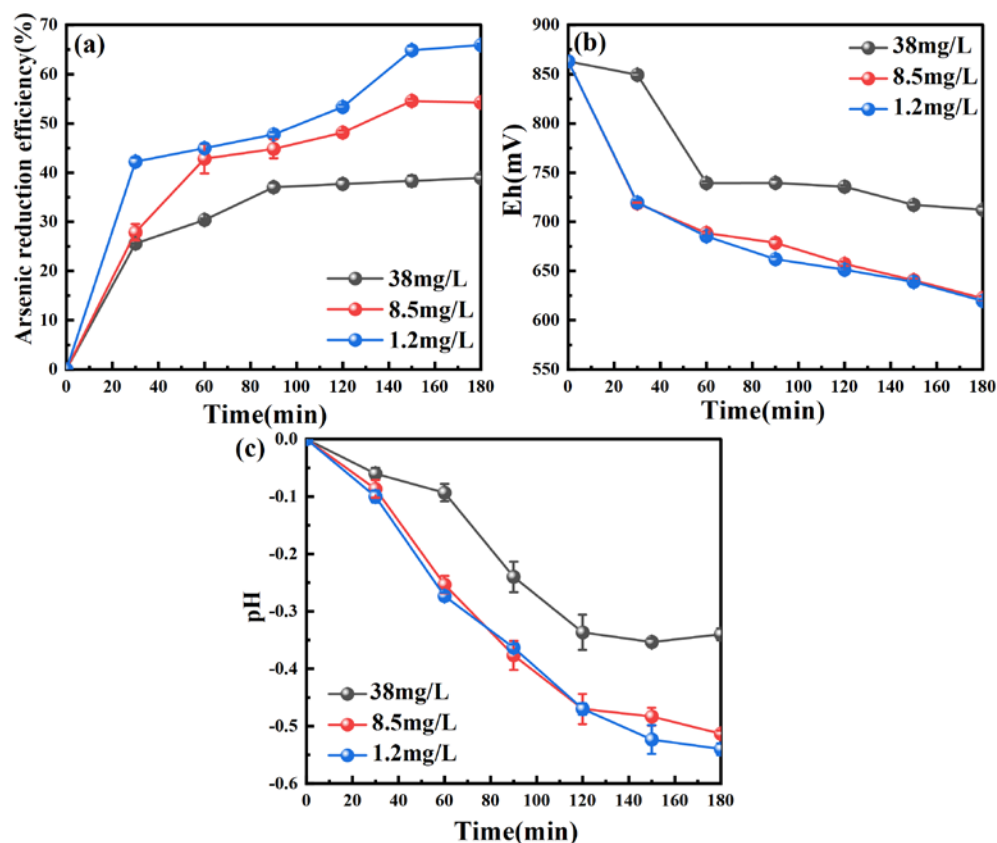


Figure 2. Effect of dissolved oxygen on (a) the As reduction efficiency, (b) solution potential (Eh), and (c) pH during the hypophosphite reduction process. Conditions: $n(H_2PO_2^-)/n(As)$ 5, initial pH 0, stirring speed 300 rpm, temperature 50 °C.

3.2.2. Effect of Hypophosphite to Arsenic Molar Ratio

The effect of the hypophosphite to arsenic molar ratio (i.e., $n(H_2PO_2^-)/n(As)$ ratio) on the recycling of As from the wastewater is shown in Figure 3. The hypophosphite concentration was found to have a significant effect on the As reduction efficiency. With the increase in the $n(H_2PO_2^-)/n(As)$ ratio from 5 to 10, the As reduction efficiency rose constantly from 54.80% to 91.61%; the further increase in $n(H_2PO_2^-)/n(As)$ ratio from 10 to 12 basically could not enhance the As reduction efficiency. The variation of Eh in Figure 3b indicates that the Eh descended with the reduction process under all $n(H_2PO_2^-)/n(As)$ ratios. The

rise of $n(\text{H}_2\text{PO}_2^-)/n(\text{As})$ ratio led to a decrease in Eh levels due mainly to the reaction of hypophosphite with Fe^{3+} (Equation (2)). Consistent with the change of E, the pH also declined, and its level was continually reduced with the increase in the $n(\text{H}_2\text{PO}_2^-)/n(\text{As})$ ratio from 5 to 7 as a result of the enhanced formation of H^+ (Equation (2)). Little change in the pH level occurred when the $n(\text{H}_2\text{PO}_2^-)/n(\text{As})$ ratio was greater than 7 (i.e., 9–11), which likely results from reaching an equilibrium of Equation (2).

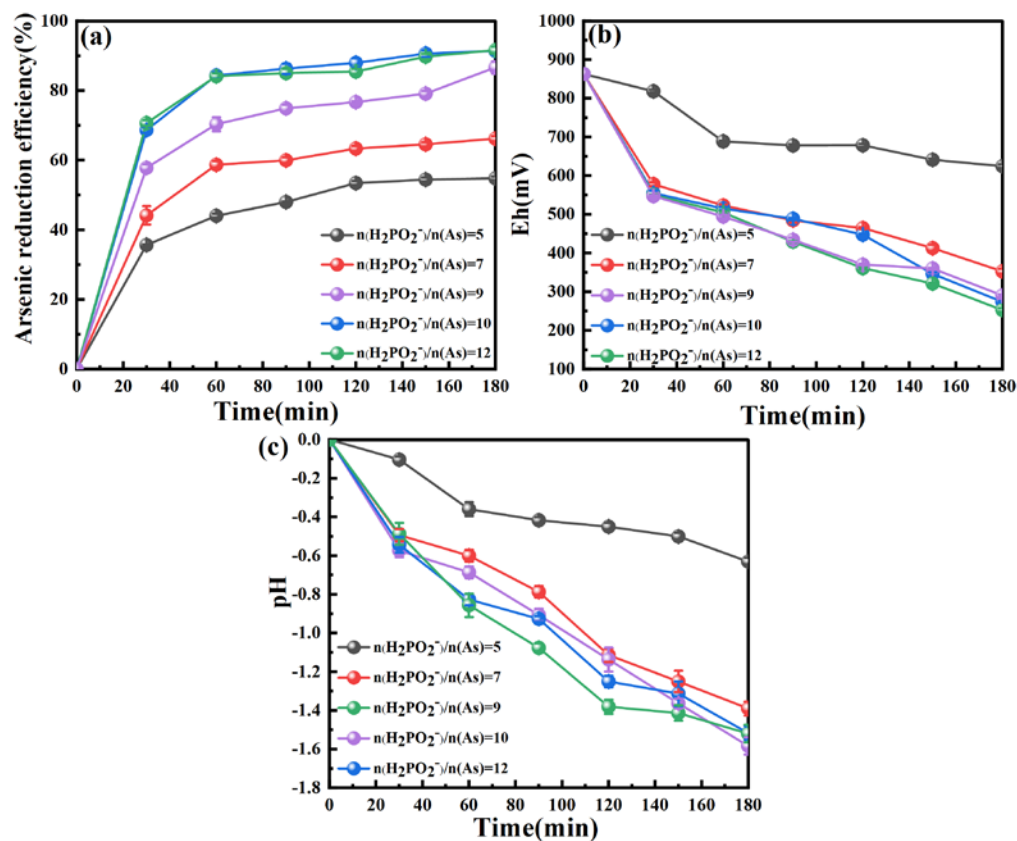


Figure 3. Effect of hypophosphite to arsenic molar ratio on (a) the As reduction efficiency, (b) Eh and (c) pH during the hypophosphite reduction process. Conditions: initial pH 0, stirring speed 300 rpm, O_2 concentration 1.2 mg/L, temperature 50 °C.

3.2.3. Effect of pH

As(V) needs to be reduced to As(IV) (H_2AsO_3 or H_4AsO_4). Then, As(IV) is reduced to As(III) by $\text{H}\bullet$ or through its disproportionation [25]. The reaction of As(V) in aqueous solution can be regarded as a complex formation between AsO_4^{3-} and H^+ [26], which is more difficult to directly reduce to As^0 from the solution than As(III) [27]. The concentration of hydrogen ion (pH) played an important role in the reduction of As(III) by As(V). The pH of the solution in the reduction process is studied. As shown in Figure 4, the As reduction efficiency was influenced noticeably by the initial pH (from 1 to -1). When the initial pH declined from 1 to -0.5 , both the reduction rate and efficiency of As increased with the reduction process. Once the initial pH was lower than -0.5 , i.e., -0.6 , the As reduction efficiency was reduced at the initial stage (30 min) of the reduction process, but afterwards it would steadily increase and reach a higher As efficiency (90.73%) than that obtained at the initial pH of 0 (88.89%) after 180 min. It is interesting that the further decrease in the initial pH (i.e., -1) would cause a deterioration for the reduction process; the As reduction rate and ratio both started to descend. The reason for this phenomenon is unclear at this stage, which requires further investigation in the future.

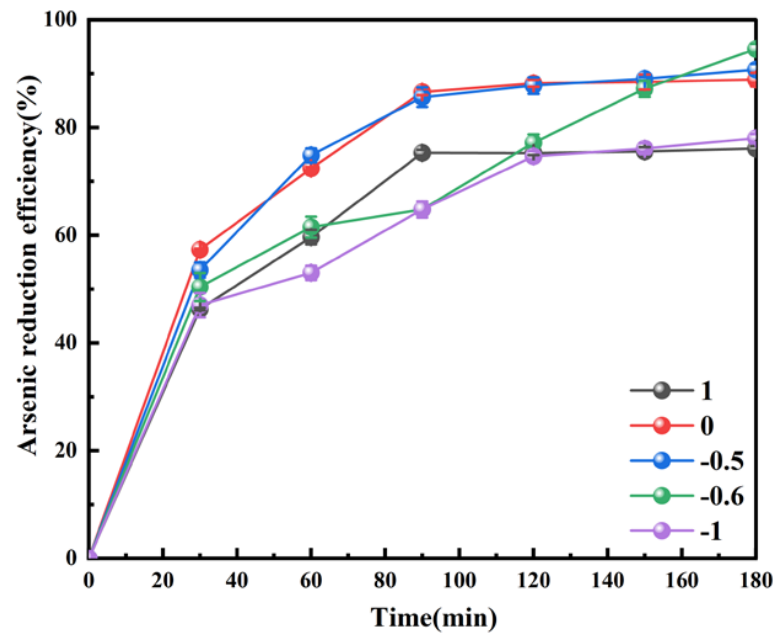


Figure 4. Effect of initial pH on the As reduction efficiency during the hypophosphite reduction process. Conditions: $n(\text{H}_2\text{PO}_2^-)/n(\text{As})$ 10, stirring speed 300 rpm, O_2 concentration 1.2 mg/L, temperature 50 °C.

3.2.4. Effect of Temperature

The temperature commonly has a significant impact on chemical reactions [28]. The effect of temperature on the hypophosphite reduction process was also investigated, as shown in Figure 5. It was found that the increase in temperature is beneficial to the recycling of As from the wastewater. At lower temperatures of 25 °C and 40 °C, the efficacy of hypophosphite reduction was much worse than that under higher temperatures (50–80 °C). In addition, the As reduction efficiency was constantly increased from 25.52% to 99.42% after 180 min with the temperature increase from 25 °C to 80 °C.

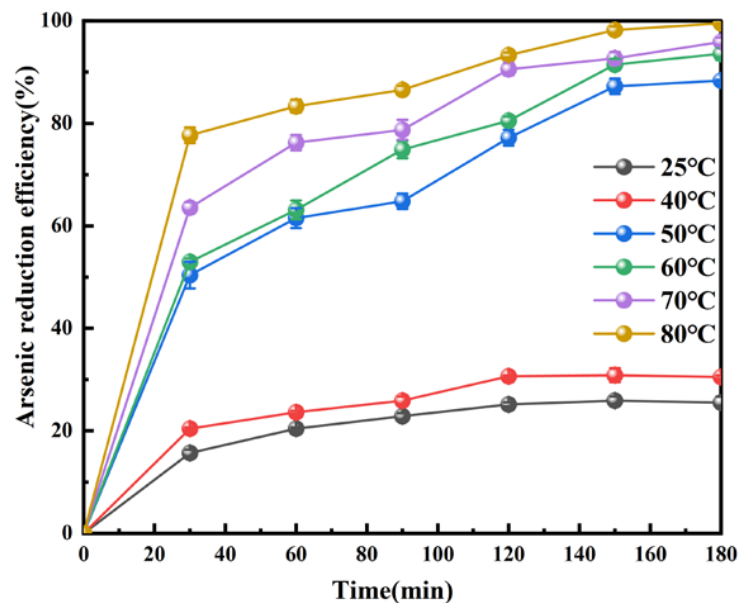


Figure 5. Effect of temperature on the As reduction efficiency during the hypophosphite reduction process. Conditions: $n(\text{H}_2\text{PO}_2^-)/n(\text{As})$ 10, initial pH −0.6, stirring speed 300 rpm, O_2 concentration 1.2 mg/L.

3.2.5. Effect of Time

The reduction is carried out under heating conditions to minimize energy consumption, and the reaction time is also studied. Under the optimal conditions of $n(\text{H}_2\text{PO}_2^-)/n(\text{As})$ 10, initial pH -0.6 , O_2 concentration 1.2 mg/L , temperature $80 \text{ }^\circ\text{C}$, the change of As reduction efficiency with reaction time was investigated as shown in Figure 6. The As reduction efficiency increased fast in the initial 90 min to 93.95%, and then it rose slowly to 99.61% after 180 min. Afterwards ($>180 \text{ min}$), the As reduction efficiency kept basically unchanged.

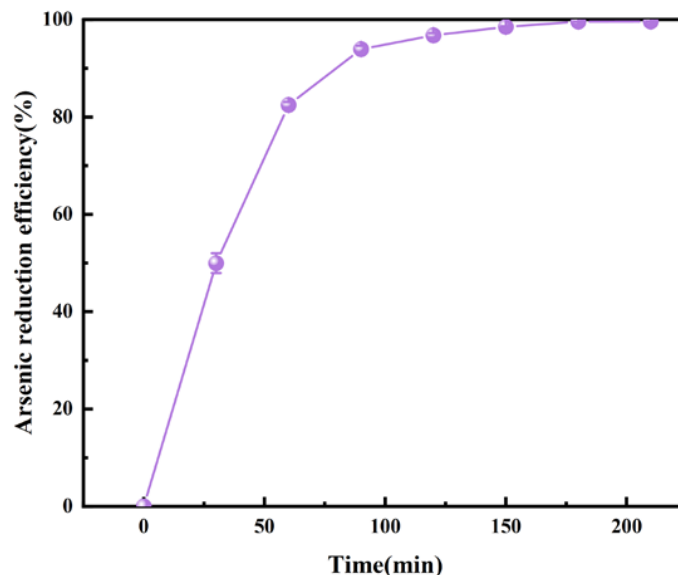


Figure 6. Variation of the As reduction efficiency during the hypophosphite reduction process under the conditions of $n(\text{H}_2\text{PO}_2^-)/n(\text{As})$ 10, initial pH -0.6 , stirring speed 300 rpm, O_2 concentration 1.2 mg/L , temperature $80 \text{ }^\circ\text{C}$.

3.3. Kinetics of the Hypophosphite Reduction Process

3.3.1. Reaction Order of Hypophosphite

Under the optimal conditions obtained from Section 3.2, the reaction order of hypophosphite concentration on the reduction of As from the acidic As-containing wastewater was investigated, as shown in Figure 7. The order of the reaction is calculated by the differential method. The logarithm of the slope of the fitted curve in Figure 7a is the vertical coordinate of Figure 7b, and the logarithm of the concentration of hypophosphite in different concentrations is the horizontal coordinate of Figure 7b. The reaction order was obtained by fitting the scatter plot.

Figure 7a shows the fitting curves that can provide the reaction rates (r) for the hypophosphate reduction process (i.e., the As reduction efficiency) at the initial stage under different hypophosphite concentrations. By taking the logarithm for the chemical reaction rate equation of $r = kC^n$, Equation (8) was obtained. The fitting curve for the relationship between the r values and the hypophosphite concentrations in Figure 7a is further shown in Figure 7b in the form of $\lg r$ vs. $\lg[\text{H}_2\text{PO}_2^-]$. The obtained slope of this fitting curve was 0.6399 (Figure 7b), i.e., the reaction order of the hypophosphite concentration. The value of this reaction order explains why the hypophosphite concentration has a crucial impact on the recycling of As from the acidic As-containing wastewater.

$$\lg r = n \lg C + \lg k \quad (8)$$

r : reaction rate

n : reaction order

C : H_2PO_2^- concentration

k : reaction rate constant

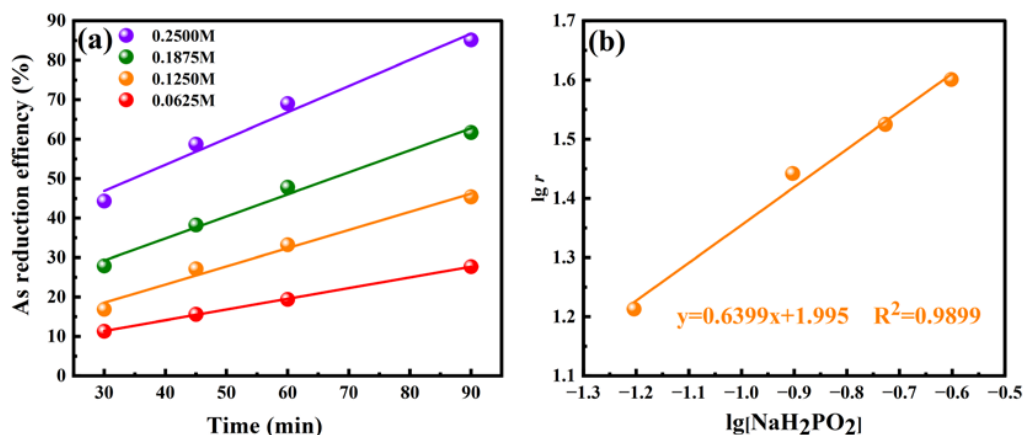


Figure 7. Fitting curves showing (a) the effect of hypophosphite concentration on the As reduction efficiency and (b) the relationship between the rate of As reduction efficiency (r) and the hypophosphite concentration in the initial stage of the reduction process. Conditions: initial pH -0.6 , stirring speed 300 rpm, O₂ concentration 1.2 mg/L, and temperature 80 °C.

3.3.2. Activation Energy

The reaction rate calculated by the four lines in Figure 8a is the reduction rate constant r of arsenic at different temperature conditions. The equation $y = -4.1287x + 15.655$ can be obtained by plotting $\ln r$ to $1/T$, as shown in Figure 7b. According to the Arrhenius equation (Equation (9)), the apparent activation energy (E_a) of arsenic precipitation can be obtained as 34.33 kJ/mol, which is between 20 and 40 kJ/mol, indicating that this process is a mixed-controlled process.

$$\ln r = \frac{-E_a}{RT} + \ln A \tag{9}$$

- r : reaction rate
- R : molar gas constant ($J \cdot mol^{-1} \cdot K^{-1}$)
- T : temperature (K)
- E_a : activation energy (kJ/mol)
- A : pre exponential factor

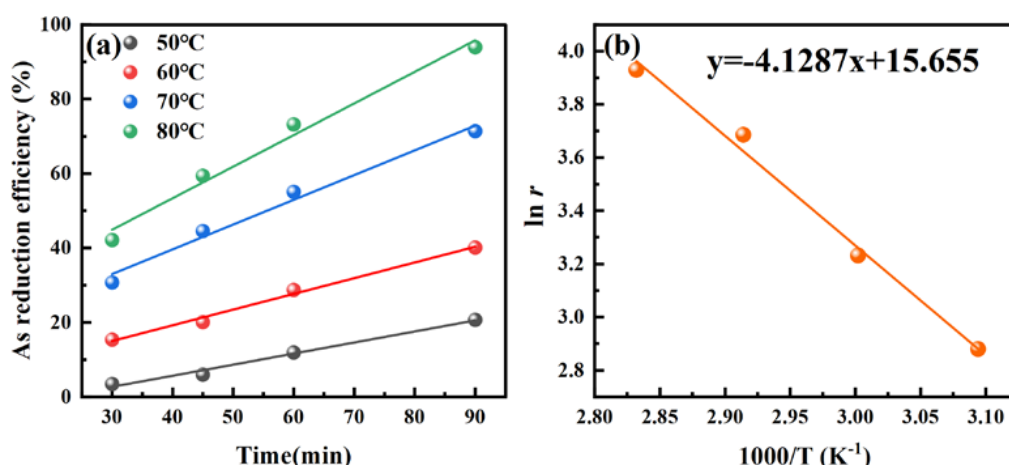


Figure 8. Fitting curves showing (a) the effect of temperature on the As reduction efficiency and (b) the relationship between $\ln r$ and $1/T$. Conditions: H₂PO₂⁻ concentration 0.2500 M, initial pH -0.6 , stirring speed 300 rpm, O₂ concentration 1.2 mg/L.

3.4. Characterization of the Elemental Arsenic Product

X-ray diffraction analysis was carried out on the arsenic precipitate collected from the reduction process under optimal experimental conditions, and the analysis result is shown in Figure 9.

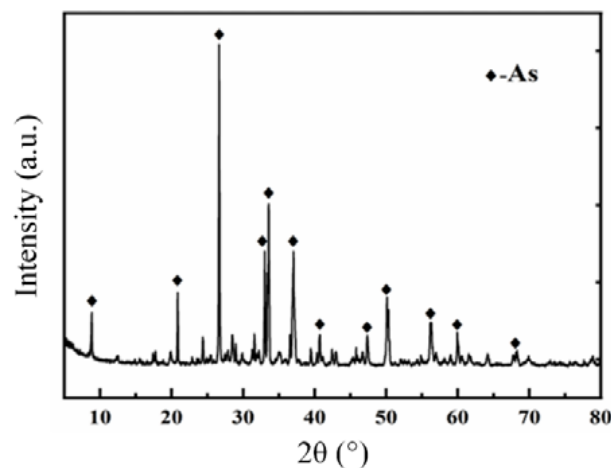


Figure 9. XRD pattern of the product.

Figure 9 shows that the attained arsenic precipitate is a pure elemental arsenic product. Its purity was further confirmed by ICP-OES; this As₀ product was shown to have an As purity of 98.5%. Consistent with the thermodynamic analysis (Section 3.1), the reduction of arsenate/arsenite by the hypophosphite achieves high-value-added pure arsenic without the formation of Fe⁰.

3.5. Reuse of the As-Containing Wastewater after Hypophosphite Reduction as Biological Culture Medium

After recycling As from the As-containing wastewater via hypophosphite reduction under optimal conditions, the main composition of the obtained wastewater was detected, as shown in Table 2. The total content of the As (As³⁺ and As⁵⁺) that is inhibitory for bacterial growth was found to be as low as 0.011 g/L. In addition, the energy substances Fe²⁺ (5.591 g/L) and PO₄³⁻ (24.361 g/L) for the reproduction of bacteria were contained in the wastewater. Therefore, the hypophosphite-reduced wastewater was reused as the culture medium for bacteria, i.e., *A. ferrooxidans*. The relevant results are shown in Figure 10.

Table 2. Composition of arsenic-containing wastewater content (g/L).

Element	Fe ²⁺	Fe ³⁺	As ³⁺	As ⁵⁺	PO ₄ ³⁻
Content	5.591	0.003	0.003	0.007	24.367

Comparing Figure 10a with b, the jarosite with a yellow color was found to form during the bacteria acclimation process, which is indicative of the propitious growth and reproduction of *A. ferrooxidans*. Figure 10c shows the growth curves of *A. ferrooxidans* in the 9K culture medium and hypophosphite reduced wastewater. The two curves with little difference confirm the success of the reuse of hypophosphite-reduced wastewater as a bacterial culture medium. The SEM image of the bacteria presented in Figure 10d further supports the above success. The results showed that the wastewater could be used as a culture medium for bacterial growth compared with 9K medium.

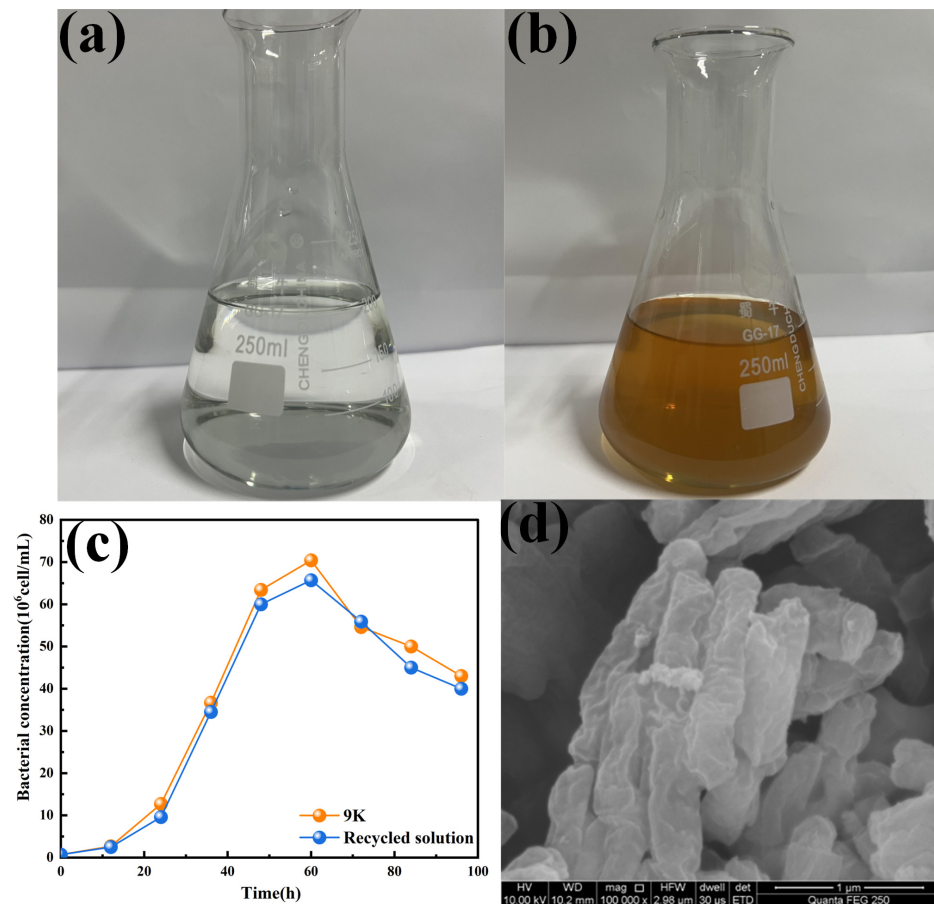


Figure 10. Photographs showing the hypophosphite reduced wastewater (a) before and (b) after 9 h bacterial acclimation. (c) Bacterial growth curves of *A. ferrooxidans* in the 9K culture medium and hypophosphite reduced wastewater. (d) SEM image of *A. ferrooxidans* in the hypophosphite reduced wastewater.

3.6. Hypophosphite Reduction Mechanisms for As Recycling from the Acidic As-Containing Wastewater

Based on the above thermodynamic analysis and experimental and analytical results, the possible mechanisms for the recycling of As from the acidic As-containing wastewater by hypophosphite reduction were proposed as shown in Figure 11. When excessive hypophosphite (H_2PO_2^-) was added to the acidic As-containing wastewater, the H_2PO_2^- was readily protonated and converted to the form of hypophosphorous acid (H_3PO_2). The formed H_3PO_2 with a high reducibility would react preferentially with Fe^{3+} , which has a strong oxidizability, producing H_3PO_4 and Fe^{2+} . The excessive H_3PO_2 also reacted with the oxidative As-containing oxyanions, i.e., H_3AsO_4 , H_3AsO_3 , and H_2AsO_2^+ , to reduce them as elemental As. H_3AsO_3 and H_2AsO_2^+ could be directly reduced to the elemental As, while H_3AsO_4 was likely to be first reduced as $\text{H}_3\text{AsO}_3/\text{H}_2\text{AsO}_2^+$, which was then reduced as the elemental As. The redox couples of $\text{H}_3\text{PO}_4/\text{H}_3\text{PO}_3$ and $\text{H}_3\text{PO}_3/\text{H}_3\text{PO}_2$ play a pivotal role in the above redox reaction process. H_3PO_2 converts Fe^{3+} and $\text{H}_3\text{AsO}_4/\text{H}_3\text{AsO}_3/\text{H}_2\text{AsO}_2^+$ separately to Fe^{3+} and As^0 , and simultaneously itself becomes H_3PO_4 finally. The removal and recycling of the As from the solution eliminates the adverse impact of As on bacterial growth; the formed Fe^{2+} and H_3PO_4 can be used as energy substances for bacterial growth.

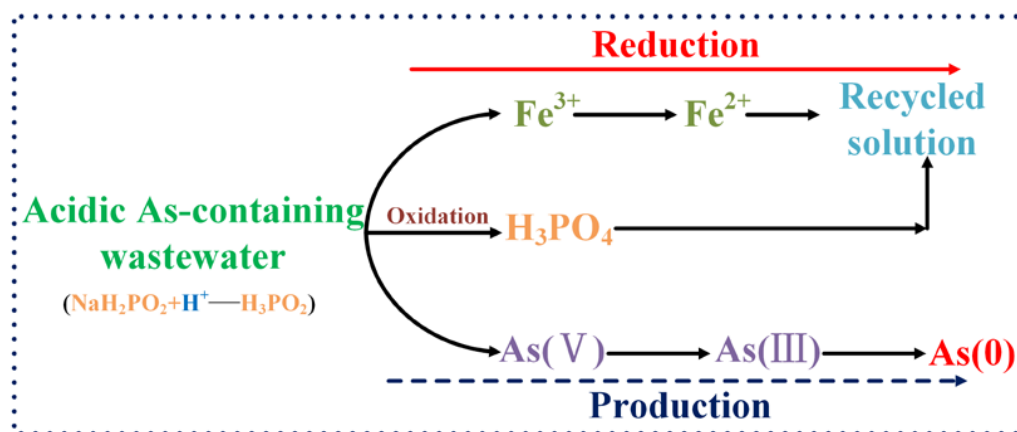


Figure 11. Schematic diagram of the mechanisms for As recycling from the acidic As-containing wastewater by hypophosphite reduction.

4. Conclusions

This paper puts forward a novel eco-friendly method of one-step hypophosphite reduction for the treatment of acidic As-containing wastewater. This method realizes the recovery of elemental arsenic, and compared with other methods, the treated solution can be used as a bacterial medium to reuse waste water. Thermodynamic analysis suggests the theoretical feasibility of the reduction of As(V)/As(III) by H_2PO_2^- or H_3PO_2 to As^0 with no formation of Fe^0 in acidic solutions. Consistent with the thermodynamic prediction, the experimental results showed that hypophosphite can effectively reduce the As from its acidic wastewater as the As^0 . The optimal conditions were found to be $n(\text{H}_2\text{PO}_2^-)/n(\text{As})$ 10, initial pH -0.6 , stirring speed 300 rpm, anaerobic environment (e.g., O_2 concentration 1.2 mg/L), time 180 min, and temperature 80°C , under which 99.61% of the As reduction efficiency was achieved. XRD analysis confirmed that the obtained solid product was elemental arsenic, and its purity was identified of reaching 98.5%. Kinetic results showed that the reaction order of H_2PO_2^- concentration was 0.64 and the activation energy was 34.33 kJ/mol, suggesting that the reduction of As(V)/As(III) by H_2PO_2^- to As^0 was a mixed control process. Wastewater recycling results showed that after recovering As, the wastewater could be reused as a bacterial culture medium. The one-step hypophosphite reduction approach proposed in this paper is eco-friendly and feasible for removing and simultaneously recovering the As from acidic As-containing wastewater in the form of high-value-added As^0 , which may have a great potential for practical application.

Author Contributions: Conceptualization, S.Z. and Q.L.; methodology, Q.L.; software, Y.Z.; validation, S.Z. and Q.L.; formal analysis, X.L. and S.Z.; data curation, Y.L.; writing—original draft preparation, S.Z. and Q.L.; writing—review and editing, X.L.; visualization, Y.Y. All authors have read and agreed to the published version of the manuscript.

Funding: We gratefully acknowledge the supports from the Hunan Provincial Natural Science Foundation of China (Grant No. 2023JJ40760), the National Key Research and Development Program of China (Grant No. 2023YFC2907801), the National Natural Science Foundation of China (Grant No. 52104256), and the Shandong Provincial Natural Science Foundation of China (Grant No. ZR2021QE023).

Data Availability Statement: The original contributions presented in the study are included in the article, further inquiries can be directed to the corresponding author.

Conflicts of Interest: Xiaoliang Liu was employed by the company Changsha Research Institute of Mining and Metallurgy Co. The remaining authors declare that the research was conducted in the absence of any commercial or financial relationships that could be construed as a potential conflict of interest.

References

1. Zhou, J.; Chen, S.; Liu, J.; Frost, R.L. Adsorption kinetic and species variation of arsenic for As(V) removal by biologically mackinawite (FeS). *Chem. Eng. J.* **2018**, *354*, 237–244. [[CrossRef](#)]
2. Zhang, Q.; Xia, H.; Xu, Y.; Jiang, G.; Cai, W.; Zhang, L. Mechanism of removal of toxic arsenic (As) from zinc sulfate solution by ultrasonic enhanced neutralization with zinc roasting dust. *Sep. Purif. Technol.* **2023**, *322*, 124258. [[CrossRef](#)]
3. Wu, J.; Li, Z.; Huang, D.; Liu, X.; Tang, C.; Parikh, S.J.; Xu, J. A novel calcium-based magnetic biochar is effective in stabilization of arsenic and cadmium co-contamination in aerobic soils. *J. Hazard. Mater.* **2020**, *387*, 122010. [[CrossRef](#)] [[PubMed](#)]
4. Siddiqui, S.I.; Naushad, M.; Chaudhry, S.A. Promising prospects of nanomaterials for arsenic water remediation: A comprehensive review. *Process Saf. Environ. Prot.* **2019**, *126*, 60–97. [[CrossRef](#)]
5. Tabelin, C.B.; Sasaki, R.; Igarashi, T.; Park, I.; Tamoto, S.; Arima, T.; Ito, M.; Hiroyoshi, N. Simultaneous leaching of arsenite, arsenate, selenite and selenate, and their migration in tunnel-excavated sedimentary rocks: I. Column experiments under intermittent and unsaturated flow. *Chemosphere* **2017**, *186*, 558–569. [[CrossRef](#)] [[PubMed](#)]
6. Igarashi, T.; Herrera, P.S.; Uchiyama, H.; Miyamae, H.; Iyatomi, N.; Hashimoto, K.; Tabelin, C.B. The two-step neutralization ferrite-formation process for sustainable acid mine drainage treatment: Removal of copper, zinc and arsenic, and the influence of coexisting ions on ferritization. *Sci. Total Environ.* **2020**, *715*, 136877. [[CrossRef](#)] [[PubMed](#)]
7. Chou, W.-C.; Chio, C.-P.; Liao, C.-M. Assessing airborne PM-bound arsenic exposure risk in semiconductor manufacturing facilities. *J. Hazard. Mater.* **2009**, *167*, 976–986. [[CrossRef](#)] [[PubMed](#)]
8. Melkonian, S.; Argos, M.; Pierce, B.L.; Chen, Y.; Islam, T.; Ahmed, A.; Syed, E.H.; Parvez, F.; Graziano, J.; Rathouz, P.J.; et al. A Prospective Study of the Synergistic Effects of Arsenic Exposure and Smoking, Sun Exposure, Fertilizer Use, and Pesticide Use on Risk of Premalignant Skin Lesions in Bangladeshi Men. *Am. J. Epidemiol.* **2011**, *173*, 183–191. [[CrossRef](#)] [[PubMed](#)]
9. Alka, S.; Shahir, S.; Ibrahim, N.; Ndejiko, M.J.; Vo, D.-V.N.; Abd Manan, F. Arsenic removal technologies and future trends: A mini review. *J. Clean. Prod.* **2021**, *278*, 123805. [[CrossRef](#)]
10. Cermikli, E.; Sen, F.; Altioek, E.; Wolska, J.; Cyganowski, P.; Kabay, N.; Bryjak, M.; Arda, M.; Yuksel, M. Performances of novel chelating ion exchange resins for boron and arsenic removal from saline geothermal water using adsorption-membrane filtration hybrid process. *Desalination* **2020**, *491*, 114504. [[CrossRef](#)]
11. Sanchez, J.; Butter, B.; Chavez, S.; Riffo, L.; Basaez, L.; Rivas, B.L. Quaternized hydroxyethyl cellulose ethoxylate and membrane separation techniques for arsenic removal. *Desalination Water Treat.* **2016**, *57*, 25161–25169. [[CrossRef](#)]
12. Zhu, N.; Yan, T.; Qiao, J.; Cao, H. Adsorption of arsenic, phosphorus and chromium by bismuth impregnated biochar: Adsorption mechanism and depleted adsorbent utilization. *Chemosphere* **2016**, *164*, 32–40. [[CrossRef](#)] [[PubMed](#)]
13. Cheng, G.; Zhang, M.; Lu, Y.; Zhang, H.; Von Lau, E. New insights for improving low-rank coal flotation performance via emulsified waste fried oil collector. *Fuel* **2024**, *357*, 129925. [[CrossRef](#)]
14. Wang, J.; Liu, J.; Peng, X.; He, M.; Hu, X.; Zhao, J.; Zhu, F.; Yang, X.; Kong, L. Reductive removal of As(V) and As(III) from aqueous solution by the UV/ sulfite process: Recovery of elemental arsenic. *Water Res.* **2022**, *223*, 118981. [[CrossRef](#)] [[PubMed](#)]
15. Feng, Z.; Ning, Y.; Yang, S.; Yu, J.; Ouyang, W.; Li, Y. A novel strategy for arsenic removal from acid wastewater via strong reduction processing. *Environ. Sci. Pollut. Res.* **2023**, *30*, 43886–43900. [[CrossRef](#)] [[PubMed](#)]
16. Li, Q.; Tian, Y.; Zhen, C.; Li, Z. Thermodynamic analysis and experiment of arsenic recovery from waste liquid of biological oxidation gold extraction. *Environ. Chem.* **2011**, *30*, 851–855.
17. Chen, H.; Ding, L.; Zhang, K.; Chen, Z.; Lei, Y.; Zhou, Z.; Hou, R. Preparation of chemically reduced graphene using hydrazine hydrate as the reduction agent and its NO₂ sensitivity at room temperature. *Int. J. Electrochem. Sci.* **2020**, *15*, 10231–10242. [[CrossRef](#)]
18. Qian, D.-W.; Yang, J.; Wang, G.-W.; Yang, S.-D. Nickel-Catalyzed Sodium Hypophosphite-Participated Direct Hydrophosphonylation of Alkyne toward H-Phosphinates. *J. Org. Chem.* **2023**, *88*, 3539–3554. [[CrossRef](#)] [[PubMed](#)]
19. Dechdacho, P.; Howard, S.; Hershey, R.L.; Parashar, R.; Perez, L.J. Effective removal of arsenic from contaminated groundwater using an iron-based metal-organic framework. *Environ. Technol. Innov.* **2023**, *32*, 103406. [[CrossRef](#)]
20. Zhang, Y.; Li, Q.; Liu, X.; Yin, H.; Yang, Y.; Xu, B.; Jiang, T.; He, Y. The catalytic effect of copper ion in the bioleaching of arsenopyrite by *Acidithiobacillus ferrooxidans* in 9K culture medium. *J. Clean. Prod.* **2020**, *256*, 120391. [[CrossRef](#)]
21. Deng, S.; Gu, G.; Xu, B.; Li, L.; Wu, B. Surface characterization of arsenopyrite during chemical and biological oxidation. *Sci. Total Environ.* **2018**, *626*, 349–356. [[CrossRef](#)] [[PubMed](#)]
22. Chen, H.-R.; Zhang, D.-R.; Li, Q.; Nie, Z.-Y.; Pakostova, E. Release and fate of As mobilized via bio-oxidation of arsenopyrite in acid mine drainage: Importance of As/Fe/S speciation and As(III) immobilization. *Water Res.* **2022**, *223*, 118957. [[CrossRef](#)] [[PubMed](#)]
23. Karamanev, D.G.; Nikolov, L.N.; Mamatarikova, V. Rapid simultaneous quantitative determination of ferric and ferrous ions in drainage waters and similar solutions. *Miner. Eng.* **2002**, *15*, 341–346. [[CrossRef](#)]
24. Lovley, D.R.; Phillips, E.J. Rapid assay for microbially reducible ferric iron in aquatic sediments. *Appl. Environ. Microbiol.* **1987**, *53*, 1536–1540. [[CrossRef](#)] [[PubMed](#)]
25. Kong, L.; Zhao, J.; Hu, X.; Zhu, F.; Peng, X. Reductive Removal and Recovery of As(V) and As(III) from Strongly Acidic Wastewater by a UV/Formic Acid Process. *Environ. Sci. Technol.* **2022**, *56*, 9732–9743. [[CrossRef](#)] [[PubMed](#)]
26. Gu, K.; Li, W.; Han, J.; Liu, W.; Qin, W.; Cai, L. Arsenic removal from lead-zinc smelter ash by NaOH-H₂O₂ leaching. *Sep. Purif. Technol.* **2019**, *209*, 128–135. [[CrossRef](#)]

27. Ostermeyer, P.; Bonin, L.; Folens, K.; Verbruggen, F.; Garcia-Timmermans, C.; Verbeken, K.; Rabaey, K.; Hennebel, T. Effect of speciation and composition on the kinetics and precipitation of arsenic sulfide from industrial metallurgical wastewater. *J. Hazard. Mater.* **2021**, *409*, 124418. [[CrossRef](#)]
28. Xue, J.; Long, D.; Zhong, H.; Wang, S.; Liu, L. Comprehensive recovery of arsenic and antimony from arsenic-rich copper smelter dust. *J. Hazard. Mater.* **2021**, *413*, 125365. [[CrossRef](#)]

Disclaimer/Publisher's Note: The statements, opinions and data contained in all publications are solely those of the individual author(s) and contributor(s) and not of MDPI and/or the editor(s). MDPI and/or the editor(s) disclaim responsibility for any injury to people or property resulting from any ideas, methods, instructions or products referred to in the content.